

BVRI Surface Photometry of the Galaxy NGC 3726

A. S. Gusev^{1,2}, A. V. Zasov¹, S. S. Kaĭsin³, and D. V. Bizyaev¹

¹*Sternberg Astronomical Institute, Universitetskii pr. 13, Moscow, 119899, Russia*

²*Institute of Solid State Physics, P.O. Chernogolovka, Moscow region, 142432, Russia*

³*Special Astrophysical Observatory, Russian Academy of Sciences, Nizhniĭ Arkhyz, Karachaevo-Cherkesskaya Republic, 357147 Russia*

Received November 19, 2001; in final form, February 1, 2002

Abstract—We present *BVRI* surface photometry of the late-type spiral galaxy NGC 3627. The distributions of the color indices and extinction-independent Q indices show that the observed photometric asymmetry in the inner part of the galaxy, including the bar, is due to an asymmetric distribution of absorbing material. The bluest regions of star formation are located in a ring surrounding the bar. The background-subtracted color indices of individual blue knots are used to estimate the ages of young stellar aggregates. In combination with previously published photometric data, our measurements indicate that the R -band profile of the disk is rather flat in its inner part ($r < 50''$) and becomes steeper further from its center. We estimate the mass of the disk and dark halo by decomposing the rotation curve. The mass-to-light ratio M/L_B for the stellar disk is ≈ 1.4 . The galaxy possesses a massive dark halo; however, the mass of the disk exceeds that of the halo in the inner part of the galaxy, which displays a regular spiral structure.

© 2002 MAIK “Nauka/Interperiodica”.

1. INTRODUCTION

Here, we will analyze detailed *BVRI* photometry and the mass distribution of the fairly close spiral galaxy NGC 3726.

The SABc galaxy NGC 3726 is located at a distance of about 12 Mpc ($H_0 = 75 \text{ km s}^{-1} \text{ Mpc}^{-1}$),¹⁾ and its luminosity is comparable to that of M31. A short bar is visible in the central region of the galaxy (Fig. 1). The two inner spiral arms of the galaxy form a ring around the bar, with several branching spirals beyond it. Table 1 presents the basic parameters of NGC 3726 adopted in our study (according to the RC3 [2] and LEDA catalogs).

The galaxy has been studied over a broad range of wavelengths by numerous observers. $U'JF$ [3], RJ [4], and JHK aperture photometry [5] are available. Parameters describing the brightness distribution over the disk (assuming an exponential brightness decrease with the radius r) and bulge of the galaxy in the J and TO bands are presented in [6]. An infrared image of the central region (from the 2MASS survey) can be found in the NASA Extragalactic Database (NED), available via the internet.

A diffuse core with an emission spectrum is seen at the galactic center, and is classified as a LINER (low-ionization emission region) [7]. According to Grosbol

[8], the luminosity of the bulge in the red does not exceed 1% of the integrated luminosity of NGC 3716, and the brightness of the disk from $8''$ to $164''$ from the center falls off exponentially with a radial scale of $63''$. However, in fact, the photometric profile is not well described by this exponential relation (see below). The azimuthal brightness distribution in NGC 3726 is fairly asymmetric at both optical wavelengths [4] and in the 21 cm line [3]. The morphology of the bar was studied in [9, 10], with very different bar parameters being obtained (for example, the derived axial ratio was $b/a = 0.5$ in [9] and $b/a = 0.22$ in [10]). The

Table 1. Basic parameters of NGC 3726

Type	SABc
B_T , mag	10.90
$M_B^{0,i}$, mag	−20.37
V_{LG} , km/s	908
D , Mpc	12.1
($H_0 = 75 \text{ km s}^{-1} \text{ Mpc}^{-1}$)	
D_{25} , arcmin	6.05
i , deg	49.2
(PA), deg	10

¹⁾In [1], the distance to the UMa cluster, to which the galaxy apparently belongs, is taken to be 15.5 Mpc.

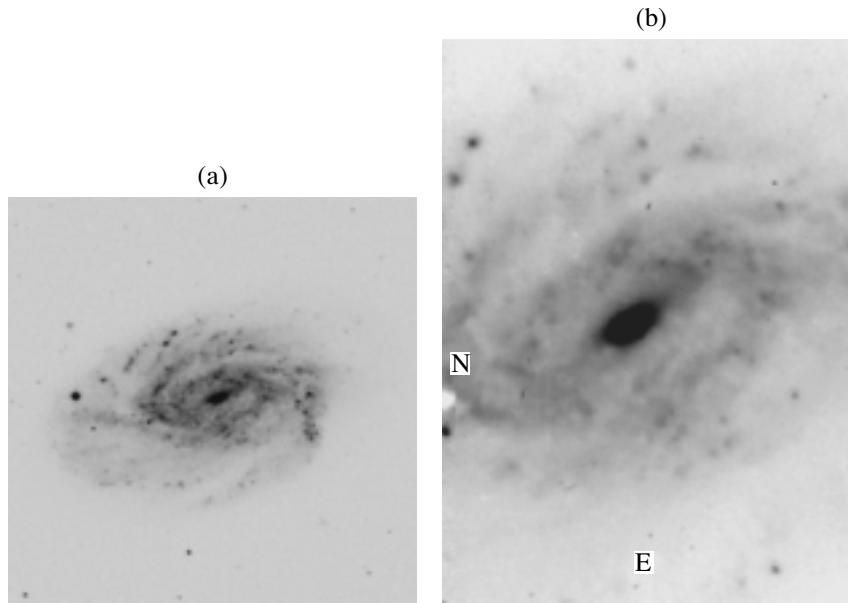


Fig. 1. (a) Digital Sky Survey image of NGC 3726 and (b) a CCD image of NGC 3726 in the V filter. The size of the region shown is (a) $6.8' \times 7.4'$ and (b) $2.4' \times 3.5'$ respectively. North is on the left and east is at the bottom.

age of the bar's population was estimated by Martinet and Friedli [11] to be 3×10^8 years (suggesting the bar is young).

The HI observations yield a mass of neutral hydrogen within a radius of $7.3'$ $M(\text{HI}) = 3.8 \times 10^9 M_{\odot}$, which makes up several percent of the total mass of the galaxy within the same radius [3]. The maximum surface density of HI is $8.5 M_{\odot}/\text{pc}^2$ and is observed $120''$ from the center of NGC 3726. Further from the center, the density of HI decreases dramatically: at a distance of $240''$, it is lower than $2.0 M_{\odot}/\text{pc}^2$.

The galaxy also displays several fairly small HII condensations, related to regions of active star formation [13]. However, the luminosity of NGC 3726 in the far infrared is low compared to that in the blue: $L_{\text{FIR}}/L_B = 0.06$ [9], indicating a moderate star-formation rate in the galaxy overall.

Here, we analyze the brightness and color-index distributions in various regions of the galaxy and model its mass distribution using the rotation curve of [1].

2. OBSERVATIONS AND REDUCTION

NGC 3726 was observed on January 22–23, 1998 with the 1-m Zeiss-1000 telescope of the Special Astrophysical Observatory in the Johnson–Cousins B, V, R, and I bands. The image size was $2.4' \times 3.5'$, with $0.28'' \times 0.37''$ per pixel. Four 600-s exposures were made in each filter, with a small shift of the frame center to decrease the effect of inhomogeneous field

sensitivity of the CCD matrix. The average seeing during the night was $3.0''$. Four standard stars from the list of Landolt [13] were observed on the same night as calibrators. The preliminary calibration was done using the ESO MIDAS package.

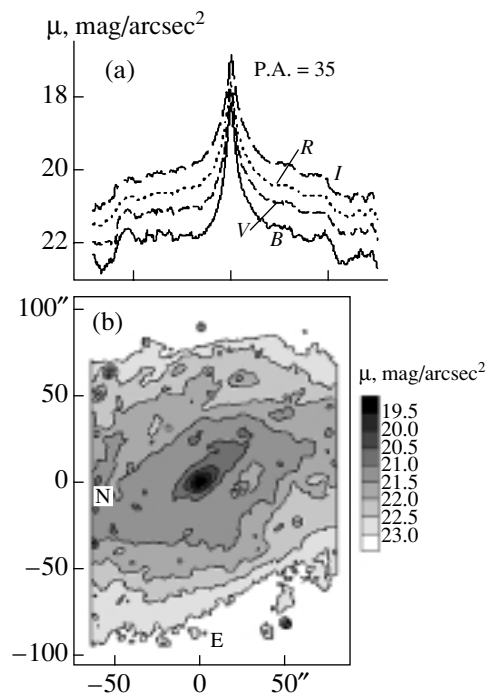


Fig. 2. (a) Photometric profiles along the major axis of NGC 3726 in B, V, R, and I along the position angle of the major axis 35° , and (b) the V isophotes of the galaxy.

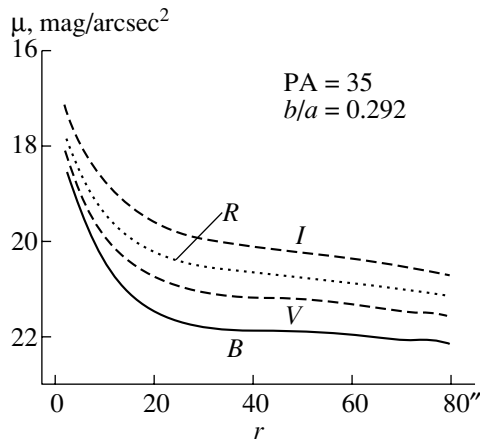


Fig. 3. Mean photometric profiles of NGC 3726 in B , V , R , and I .

The accuracy of the photometric calibration was 0.06^m in V and R , 0.12^m in B , and 0.04^m in I . We corrected both the brightness and color indices for Galactic extinction. We also introduced average corrections for the color excesses due to the inclination of the galactic disk to the line of sight (taken from the RC3 catalog [2]) for two-color diagrams and the colors of star-formation sites.

3. RESULTS

Due to the limited size of the field, we were able to study in detail only the inner region of the galaxy (Fig. 1b)—approximately $0.4D_{25}$, where D_{25} is the optical diameter. The outer regions of the disk to the north and south of the center of NGC 3726 remained beyond our field of view. Therefore, the results presented here correspond to a region with a radius of about $80''$ (≈ 5 kpc). Apart from the disk, this region also contains the bright compact bulge (with a maximum V brightness of 17.8 mag/arcsec 2), which dominates within the central $20''$ (about 1 kpc).

The brightness decrease in the core region along the major axis is asymmetric: it falls off very steeply toward the northeast, while the gradient toward the southwest is substantially smaller, especially in B (Fig. 2a). This was probably why van den Bergh [14] classified the core of NGC 3726 as a diffuse (non-star-like) object. The asymmetry is most pronounced in B and appreciably smaller in red filters, suggesting that it is related to some asymmetry in the distribution of either an absorbing medium or blue stars. We will show below that the first possibility is more likely.

The brightness of the bar of the galaxy, with a radius of about 3 kpc ($50''$), is also asymmetric. The surface brightness of the southwestern part of the bar falls off with distance exponentially, from

$\mu_V = 20.8 \pm 0.03$ mag/arcsec 2 in the central region to $\mu_V = 21.3 \pm 0.05$ mag/arcsec 2 at the periphery. The V brightness of the northeastern part of the bar is 0.3 mag/arcsec 2 lower (Figs. 2a, 2b). At the edges of the bar ($r = 50''$), the local brightness increases in the blue by 0.3 – 0.4 mag/arcsec 2 in B . The ellipticity of the bar isophotes is 0.31 ± 0.01 in B , V , and R . The position angle of the bar ($PA = 25^\circ \pm 3^\circ$) is close to that of the major axis of the disk of the galaxy as a whole.

The spiral arms emerging from the ends of the bar form a ring with inner radius 2.9 kpc ($50''$). Its azimuth-averaged surface brightness is $\mu_V = 21.2 \pm 0.2$ mag/arcsec 2 .

Figure 3 presents mean photometric profiles for the adopted disk position angle and axial ratio (the brightness is not corrected for the disk inclination). Decomposition of the profiles into the disk and bulge with its exponential profile (Table 2) indicates that, at distances $r = 26''$ – $50''$ from the center, the main contribution to R is made by the disk, with a very slow exponential decrease of the brightness (with scale $r_{\text{disk}} = 5.4 \pm 0.1$ kpc ($92'' \pm 2''$)) and a central surface brightness of $\mu_R(0) = 20.18 \pm 0.02$ mag/arcsec 2 .

The disk brightness falls off more slowly at shorter wavelengths (see Table 2). The disk of NGC 3726 extends appreciably beyond our images. We used the FITS archive of Frei *et al.* [15], which contains R photometric data obtained with the 1.1-m telescope of the Lowell Observatory, to study the R photometric profile at large r . These data are in good agreement with our within $80''$ of the center (with an accuracy of 0.06 mag/arcsec 2). The azimuthal profiles at distances from $50''$ to $150''$ of the galactic center indicate that, at large r , the disk of NGC 3726 displays a radial scale of $r_{\text{disk}} = 3.26 \pm 0.05$ kpc ($55.6'' \pm 0.9''$) and $\mu_R(0) = 20.74 \pm 0.04$ mag/arcsec 2 ; the outer region of the disk makes a transition to the inner region $40''$ – $50''$ from the center. The obtained estimate for r_{disk} is consistent with the value $58''$ found for the K band in [6].

Thus, NGC 3726 displays a brightness (density) “deficiency” in the inner part of its disk (a type II photometric profile according to Freeman [16]). In the region $r = 4''$ – $18''$ from the center occupied by the bulge, an exponential brightness decrease with the scale $r_{\text{bulge}} = 300 \pm 5$ pc ($5.11'' \pm 0.09''$) is observed; the surface brightness extrapolated to the center is $\mu_R(0) = 17.95 \pm 0.04$ mag/arcsec 2 .

NGC 3726 is rather blue. Its integrated color index corrected for the Galactic extinction is $(B - V)_0 = 0.52^m$ [17]. According to our data, the color remains blue even in the bulge region. The color indices of the bulge ($B - V = 0.5^m \pm 0.1^m$, $V - R = 0.33^m \pm$

Table 2. Photometric parameters of the components of NGC 3726

Components	Filters	Distance interval, arcsec	Characteristic scale		Central surface brightness, mag/arcsec ²
			arcsec	kpc	
Bulge	<i>B</i>	4–18	4.5 ± 0.1	0.26 ± 0.01	18.57 ± 0.06
	<i>V</i>		4.8 ± 0.1	0.28 ± 0.01	18.25 ± 0.05
	<i>R</i>		5.1 ± 0.1	0.30 ± 0.005	17.95 ± 0.04
	<i>I</i>		5.0 ± 0.1	0.30 ± 0.004	17.24 ± 0.03
Inner disk	<i>B</i>	26–50	151.0 ± 7.2	8.86 ± 0.42	21.54 ± 0.03
	<i>V</i>		111.1 ± 2.7	6.51 ± 0.16	20.76 ± 0.02
	<i>R</i>		91.9 ± 1.7	5.39 ± 0.10	20.18 ± 0.02
	<i>I</i>		72.1 ± 1.3	4.23 ± 0.08	19.50 ± 0.02
Outer disk	<i>R</i>	50–150	55.6 ± 0.9	3.26 ± 0.05	20.74 ± 0.04

Table 3. Parameters of sites of star formation

No.	Coordinates, arcsec	$(B-V)_0^i$	$(V-R)_0^i$	$(V-I)_0^i$	<i>d</i> , pc	<i>t</i> , 10 ⁶ years
1	59.3N, 0.8W	0.39	0.27	–	130	>8
2	53.8N, 24.6W	–0.03	0.00	0.32	220	5.8 ± 0.5
3	59.3N, 52.5W	–0.02	0.11	0.75	245	5.8 ± 0.6
4	53.1N, 63.5W	0.02	0.18	0.03	190	6.2 ± 0.9
5	4.4S, 63.1W	0.07	0.01	0.03	210	6.1 ± 0.9
6	22.8S, 60.2W	0.11	0.06	0.34	215	6.4 ± 0.8
7	25.7S, 29.0W	0.06	0.16	0.49	360	6.9 ± 0.2
8	46.6S, 10.0W	–0.04	0.09	0.58	170	6.6 ± 0.9
9	12.1S, 29.6E	0.02	0.01	0.19	550	5.9 ± 0.8
10	34.1S, 39.1E	0.03	–0.08	0.23	190	5 ± 2
11	39.9N, 46.8E	–0.04	–0.05	0.59	180	5.6 ± 1.9
12	6.2N, 24.6W	–0.35	–	0.10	60	<3

0.13^m, $R - I = 0.65^m \pm 0.03^m$) are comparable to those of the galactic disk (Figs. 5a–5d), suggestive of star formation in the circumnuclear region.

The color distribution in the galaxy is appreciably asymmetric. Within 2.9 kpc (50′′) from the center, the northern and eastern parts of the inner disk are, on average, redder than regions to the south and west of the core by 0.1^m in $B - V$ and 0.05^m in $V - R$ (Figs. 4a–4d). However, the “red” $R - I$ color-index distribution in the galaxy remains azimuthally symmetric (Figs. 4a, 4d). The reddest regions are the core and the inner regions of the northeastern part of the bar, where the color indices reach $B - V =$

0.8^m ± 0.1^m, $V - R = 0.60^m \pm 0.05^m$, and $R - I = 0.70^m \pm 0.05^m$ (Fig. 4a).

On average, the galaxy becomes bluer with distance from the center. However, the radial variations of $B - V$ and $V - R$ to the north and south of the core (along the major axis) differ substantially (Fig. 4a): $B - V$ decreases towards the northeast from 0.8^m ± 0.1^m to 0.5^m ± 0.1^m at the periphery, remaining essentially constant ($B - V = 0.65^m \pm 0.15^m$) toward the southwest of the center. $V - R$ behaves in a similar way (decreasing with distance from 0.60^m ± 0.05^m to 0.40^m ± 0.05^m toward the northeast and remaining constant (0.47^m ± 0.04^m) toward the southwest). However, $R - I$, which is the least

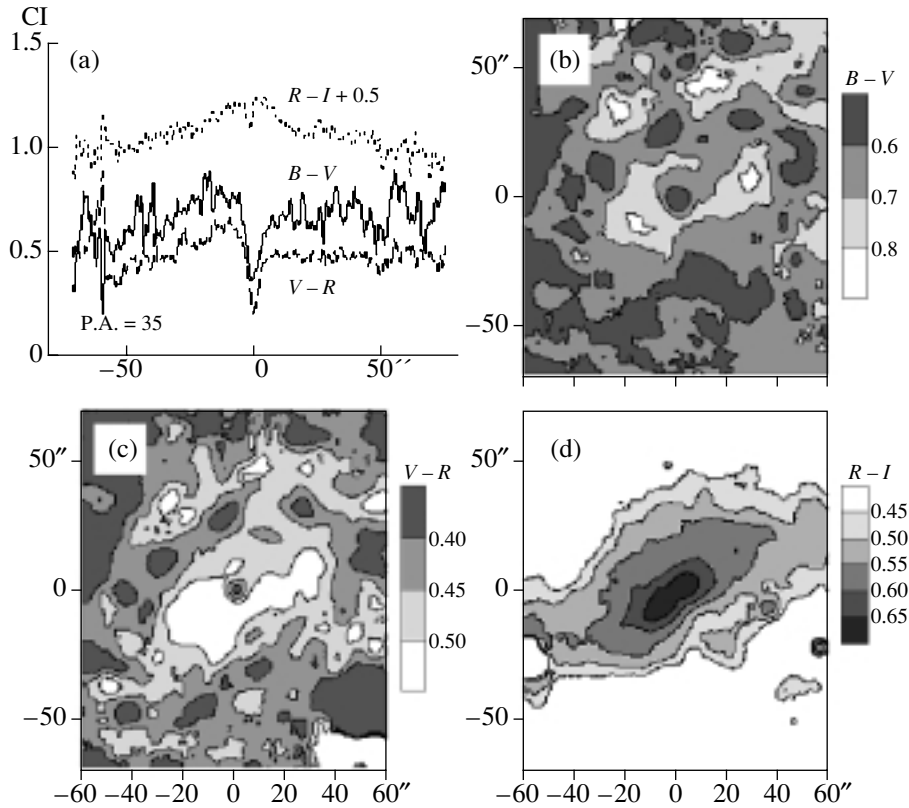


Fig. 4. (a) The color indices $B - V$, $V - R$, and $R - I$ along the major axis of NGC 3726, together with color-index maps for the galaxy in (b) $B - V$, (c) $V - R$, and (d) $R - I$.

sensitive to the presence of an absorbing medium and/or blue stars, varies almost symmetrically along the major axis of the galaxy, decreasing from $0.70^m \pm 0.05^m$ to $0.45^m \pm 0.05^m$ at the periphery (Fig. 4a). The ring of NGC 3726 is the bluest region in the galaxy. Its azimuth-averaged color indices are $B - V = 0.54^m \pm 0.06^m$, $V - R = 0.40^m \pm 0.07^m$, and $R - I = 0.46^m \pm 0.11^m$; bright local formations in the ring and the spiral arms of the outer disk are even bluer (for more detail about the sites of star formation, see Section 5).

4. PHOTOMETRIC INDICES Q

The color inhomogeneity of the galaxy, including the large-scale color asymmetry, may be due to peculiarities of the distributions of both an absorbing medium and regions of star formation. In both cases, the inhomogeneity should be most pronounced for the “blue” $B - V$ color index, as is observed. To investigate the structure of the galaxy and distinguish between these two cases, Zasov and Moiseev [18] and Bizyaev *et al.* [19] introduced a convenient photometric index Q , which combines pairs of color indices (for example, Q_{BVI} , Q_{VRI} , and so on) and is independent (ideally, at least) of selective absorption.

It is assumed that the ratios of dust-related color-excesses in different photometric bands are close to those accepted for our Galaxy.

The values of the Q parameters are primarily determined by the relative luminosities of young stars, old stars, and gas in the $H\alpha$ line; the chemical composition of the stellar population; and, in the presence of a burst of star formation, the characteristic age of the burst and the relative mass of the stars formed. As was shown in [19], Q_{BVI} is the most sensitive Q parameter to the presence of blue stars, while Q_{VRI} can be used to localize regions with intense $H\alpha$ emission in the R band. Figures 5a and 5b present maps of the Q_{BVI} and Q_{VRI} distributions in the central region of NGC 3726.

The circumnuclear region can be distinguished in these maps, together with a number of young stars, manifest as darker regions with decreased color index. The spiral arms show less contrast in the Q map (and can be distinguished even more poorly in ordinary color maps). The fraction of radiation associated with young stars is highest in the arms, and, judging from the Q_{VRI} maps, they contain the bulk of the HII regions, leading to an increase in this index. On the whole, the disk looks more symmetric in the Q_{BVI} map than in the color maps, suggesting that the color

asymmetry of the galaxy is related to the distribution of dust rather than the distribution of young stars in the disk.

5. STAR-FORMATION SITES IN THE GALAXY

We have identified 12 bright, blue star-formation regions in the ring and spiral arms of NGC 3726. Figures 6a and 6b indicate their locations in the $(B - V)_0^i - (V - R)_0^i$ and $(B - V)_0^i - (V - I)_0^i$ two-color diagrams. We estimated the color indices by subtracting the disk background from the images of these bright regions in each filter, estimating the background in the nearest vicinity of these regions. The effective ages of the sites of star formation were derived from their locations in the two-color diagrams by using evolutionary tracks of aging stellar systems with solar chemical composition which were obtained with the PEGASE code available via the internet (dotted line). The solid line indicates the mean position of the dependence along which galaxies of various morphological types are located, according to the data of Buta and Williams [20].

The columns in Table 3 present the derived parameters of these objects: their coordinates from the center of the galaxy in arcseconds (2); $(B - V)_0^i$, $(V - R)_0^i$, and $(V - I)_0^i$ color indices (3–5), the diameter of the region in parsecs (6), and its estimated age (7). The sizes of most of the star-formation sites in NGC 3726 are 150–250 pc. In the hierarchical star-formation scale suggested by Efremov [21], such sizes are typical of stellar aggregates. All the star-formation sites (except for 1, 12) lie close to each other in the two-color diagrams, in the region corresponding to stellar systems with ages of 5–7 million years (Figs. 6a, 6b). The color indices of the faint regions 1 and 12 have large uncertainties, and their ages cannot be estimated reliably from our data.

6. KINEMATICS OF THE GALAXY AND MASSES OF THE COMPONENTS

The rotation curve of the galaxy $V(r)$ derived from observations of the HI line is presented in [1]. The curve $V(r)$ displays a rather unusual shape, having a maximum at $r \approx 6$ kpc (which is obviously beyond the bright bulge, for the adopted distance to the galaxy) and then increasing again somewhat more slowly at the periphery.

The inner increasing part of the rotation curve must be due to the disk, since the bulge of the galaxy is very small and the influence of the halo becomes important only in the outer regions of the galaxy. This fact, along with the presence of a local minimum in the rotation curve, presents a rare opportunity to

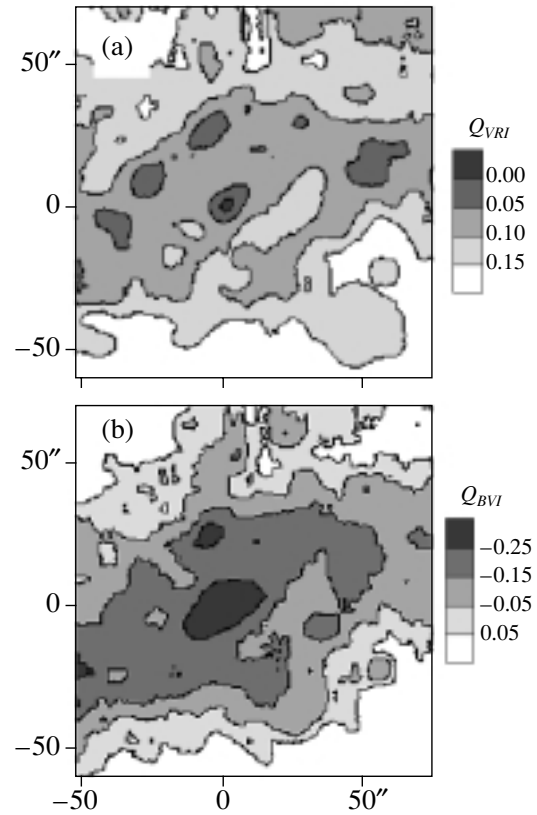


Fig. 5. Distributions of the combined parameters (a) Q_{VRI} and (b) Q_{BVI} over the disk of the galaxy.

appreciably decrease the uncertainties in the masses of the disk and halo derived by decomposing the $V(r)$ curve into corresponding components.

We will assume that the surface density of the thin disk of the galaxy matches the observed brightness distribution in the R and I bands (Table 2), varying exponentially with indices $-r/5.4$ kpc ($\approx 90''$) to $r = 2.9$ kpc ($50''$) (the inner disk) and 3.3 kpc ($57''$) for $r > 2.9$ kpc (the outer disk). Note that the photometric profile of the disk at the periphery of the galaxy ($r > 180''$) displays a rapid brightness decrease with a characteristic scale slightly larger than 1 kpc [3]; however, the disk density at this distance is so small that this steepening of the profile does not affect the rotation curve, whose shape at large distances from the center is determined by the halo.

Table 4. Masses of the components of NGC 3726

r , kpc	$M_{\text{disk}}, 10^9 M_{\odot}$	$M_{\text{halo}}, 10^9 M_{\odot}$
5	16.5	3.0
10	30.5	18.5
15	35.8	54.1

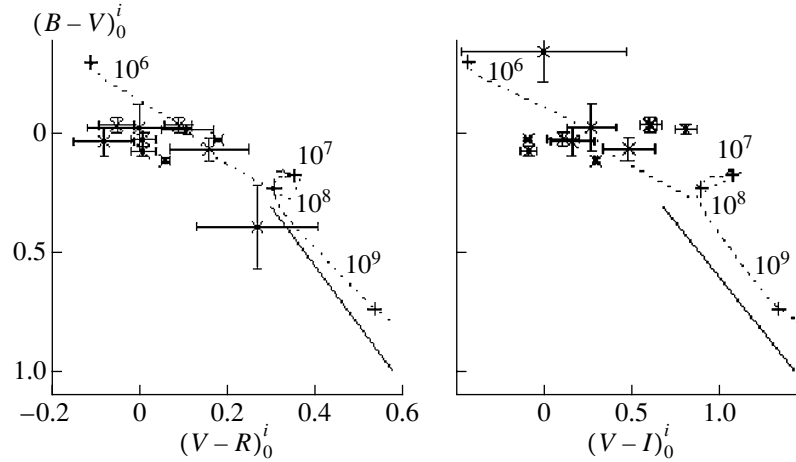


Fig. 6. $(B - V)_0^i - (V - R)_0^i$ and $(B - V)_0^i - (V - I)_0^i$ two-color diagrams for sites of star formation in the galaxy (x's). The solid line marks the mean color sequence for galaxies according to [20]. The dotted lines indicate the evolutionary tracks of a stellar system without star formation (the crosses mark positions corresponding to the ages of the system in years indicated in the diagram). The bars show the estimated errors.

In addition to the thin disk, the model includes a gaseous disk, whose surface density is assumed to be twice the HI density (to take into account the abundance of heavier elements and molecular gas); the bulge, whose density distribution is described by a King law; and a quasi-isothermal halo. We used the GR4 code written by A.N. Burlak for the modeling. Figure 7 presents the resulting decomposition of the rotation curve into components related to different parts of the galaxy.

There is no doubt that the galaxy possesses a massive dark halo (the model asymptotic velocity is about 200 km/s) responsible for the high rotational velocity at large r ; however, its contribution to the

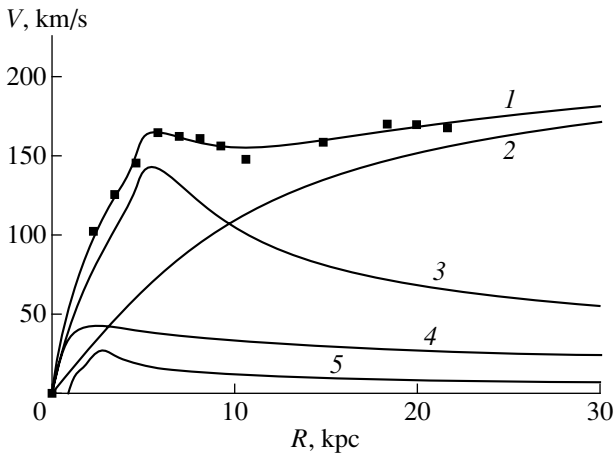


Fig. 7. Rotation curve of NGC 3726. The squares indicate the observational data and curve 1 the model curve. The components of the rotation curve related to the halo (2), disk (3), bulge (4), and gas (5) are indicated.

total mass in the region of the rotation curve maximum is insignificant. The disk and the halo masses become equal only at $r = 12\text{--}14$ kpc, so that, despite its modest total mass, the disk of NGC 3726 can be considered to be self-gravitating in the region of the bright spirals (2–10 kpc). The mass of the bulge is too small to be estimated reliably from the shape of the rotation curve.

The model explains the local minimum in the rotation curve, although the observed depth of the minimum is somewhat larger than in the model. Some large-scale, non-circular gas motions with low amplitudes may occur in this region (6–10 kpc from the center). Note that the region of the minimum corresponds to the distances from the center where the regular spiral pattern disappears and the extended asymmetric outer disk with floccular structure begins.

Table 4 presents the relative masses of the disk and halo inside spheres with radii 5, 10, and 15 kpc. The total mass of the stellar components of the galaxy is around $3.5 \times 10^{10} M_{\odot}$, which corresponds to a rather low M/L_B ratio ≈ 1.4 for the stellar population. By varying the model parameters, we estimated the uncertainty of this value to be $\pm 20\%$.

7. CONCLUSIONS

We conclude that the asymmetry of the bar and inner disk of NGC 3726 is primarily due to an asymmetric distribution of an absorbing medium. Active star formation is underway in the ring around the bar and in the core region; the colors of the brightest blue condensations corresponds to ages of 5–7 million years. The inner and outer stellar disks can be distinguished in the galaxy; the mass of the disk

dominates that of the halo out to distances $r = 10\text{--}13$ kpc, within which the arms are regular. Thus, a regular spiral structure is formed within the stellar disk of NGC 3726, which is self-gravitating; this structure loses its regularity where the contribution of the disk to the total mass no longer dominates.

ACKNOWLEDGMENTS

This work was supported by the Russian Foundation for Basic Research, project no. 01-02-17597.

REFERENCES

1. R. Sanders and M. Verheijen, *Astrophys. J.* **503**, 97 (1998).
2. G. de Vaucouleurs, A. de Vaucouleurs, H. G. Corwin, *et al.*, *Third Reference Catalogue of Bright Galaxies* (Springer-Verlag, New York, 1991).
3. B. M. H. R. Wevers, P. C. van der Kruit, and R. J. Allen, *Astron. Astrophys., Suppl. Ser.* **66**, 505 (1986).
4. C. J. Conselice, *Publ. Astron. Soc. Pac.* **109**, 1251 (1997).
5. M. Shaw, D. Axon, R. Probst, and I. Gatley, *Mon. Not. R. Astron. Soc.* **274**, 367 (1995).
6. C. Mollenhoff and J. Heidt, *Astron. Astrophys.* **368**, 16 (2001).
7. R. W. Pogge, *Astrophys. J., Suppl. Ser.* **71**, 433 (1989).
8. P. J. Grosbol, *Astron. Astrophys., Suppl. Ser.* **60**, 261 (1985).
9. P. Martin, *Astron. J.* **109**, 2428 (1995).
10. S. Chapelon, T. Contini, and E. Davoust, *Astron. Astrophys.* **345**, 81 (1999).
11. L. Martinet and D. Friedli, *Astron. Astrophys.* **323**, 363 (1997).
12. P. W. Hodge, *Astron. J.* **87**, 1341 (1982).
13. A. Landolt, *Astron. J.* **88**, 853 (1983).
14. S. van den Bergh, *Astron. J.* **110**, 613 (1995).
15. Z. Frei, P. Guhathakurta, J. E. Gunn, and J. A. Tyson, *Astron. J.* **111**, 174 (1996).
16. K. C. Freeman, *Astrophys. J.* **160**, 811 (1970).
17. P. Prugniel and P. Heraudeau, *Astron. Astrophys., Suppl. Ser.* **128**, 299 (1998).
18. A. V. Zasov and A. V. Moiseev, *Pis'ma Astron. Zh.* **24**, 677 (1998) [*Astron. Lett.* **24**, 584 (1998)].
19. D. V. Bizyaev, A. V. Zasov, and S. S. Kařsin, *Pis'ma Astron. Zh.* **27**, 254 (2001) [*Astron. Lett.* **27**, 217 (2001)].
20. R. Buta and K. L. Williams, *Astron. J.* **109**, 543 (1995).
21. Yu. N. Efremov, *Sites of Star Formation in Galaxies* [in Russian] (FM, Moscow, 1989).

Translated by K. Maslennikov